

Dust Biasing of Damped Lyman Alpha Systems: a Bayesian Analysis

Andrew Pontzen^{1*}, Max Pettini¹

¹*Institute of Astronomy, Madingley Road, Cambridge CB3 0HA, UK*

Accepted 2008 November 03. Received 2008 October 30; in original form 2008 September 01

ABSTRACT

If damped Lyman alpha systems (DLAs) contain even modest amounts of dust, the ultraviolet luminosity of the background quasar can be severely diminished. When the spectrum is redshifted, this leads to a bias in optical surveys for DLAs. Previous estimates of the magnitude of this effect are in some tension; in particular, the distribution of DLAs in the (N_{HI} , Z) (i.e. column-density – metallicity) plane has led to claims that we may be missing a considerable fraction of metal rich, high column density DLAs, whereas radio surveys do not unveil a substantial population of otherwise hidden systems.

Motivated by this tension, we perform a Bayesian parameter estimation analysis of a simple dust obscuration model. We include radio and optical observations of DLAs in our overall likelihood analysis and show that these do not, in fact, constitute conflicting constraints.

Our model gives statistical limits on the biasing effects of dust, predicting that only 7% of DLAs are missing from optical samples due to dust obscuration; at 2σ confidence, this figure takes a maximum value of 17%. This contrasts with recent claims that DLA incidence rates are underestimated by 30 – 50%. Optical measures of the mean metallicities of DLAs are found to underestimate the true value by just 0.1 dex (or at most 0.4 dex, 2σ confidence limit), in agreement with the radio survey results of Akerman et al. As an independent test, we use our model to make a rough prediction for dust reddening of the background quasar. We find a mean reddening in the DLA rest frame of $\log_{10}\langle E_{B-V} \rangle \simeq -2.4 \pm 0.6$, consistent with direct analysis of the SDSS quasar population by Vladilo et al., $\log_{10}\langle E_{B-V} \rangle = -2.2 \pm 0.1$. The quantity most affected by dust biasing is the total cosmic density of metals in DLAs, $\Omega_{Z,\text{DLA}}$, which is underestimated in optical surveys by a factor of approximately two.

Key words: quasars: absorption lines

1 INTRODUCTION

Damped Lyman alpha systems (DLAs), neutral gas with column densities $N_{\text{HI}} > 2 \times 10^{20} \text{ cm}^{-2}$ seen in absorption against more distant luminous sources (generally quasars), are of substantial interest to observational and computational cosmologists. Despite disagreement over their precise nature, they are certain to trace a set of objects which constrain our theories of galaxy formation. This is guaranteed by the simple observational fact that they contain the overwhelming majority of neutral hydrogen (a necessary precursor to molecular hydrogen and therefore star formation) over all redshifts $z > 0$ (Tytler 1987). For a review of observational and theoretical results see Wolfe et al. (2005).

One area of controversy in the interpretation of DLA observations is the extent to which biases are introduced by dust: it is possible to imagine scenarios in which certain metal rich, high column density DLAs dim their background quasars such that significant fractions are not detected in optical surveys. Early attempts at assessing the magnitude of this effect by comparing the spectral slopes of QSOs with and without intervening DLAs seemed to

suggest that estimates of important quantities such as the total density of neutral hydrogen (Ω_{DLA}) and the mean metallicity ($\langle Z \rangle$) of DLAs could be incorrect by orders of magnitude (Fall & Pei 1993, and references therein). While recent results (e.g. Murphy & Liske 2004; Ellison et al. 2005; Vladilo et al. 2008) show that the extent of dust reddening was substantially overestimated in these early works, emphasis on the observational evidence in apparent support of the obscuration scenario has shifted to the distribution of absorbers in (N_{HI} , Z) space. First noted by Boissé et al. (1998), there is a dearth of absorbers exhibiting simultaneously high N_{HI} and high Z – exactly as would be expected in a scenario invoking significant dust absorption. Recent work on such models (e.g. Vladilo & Péroux 2005) has suggested that smaller but still important effects arise from dust obscuration. In particular, a dust-induced bias has been invoked by simulators to reconcile high DLA metallicities encountered in models with the generally low values measured empirically (Cen et al. 2003; Nagamine et al. 2004).

One should be clear, however, that this interpretation is not unique – when at the tails of both N_{HI} and Z distributions, systems will anyway be rare (see Figure 1, which shows similar distributions arising from the different models described in Section 2.1).

* Email: apontzen@ast.cam.ac.uk

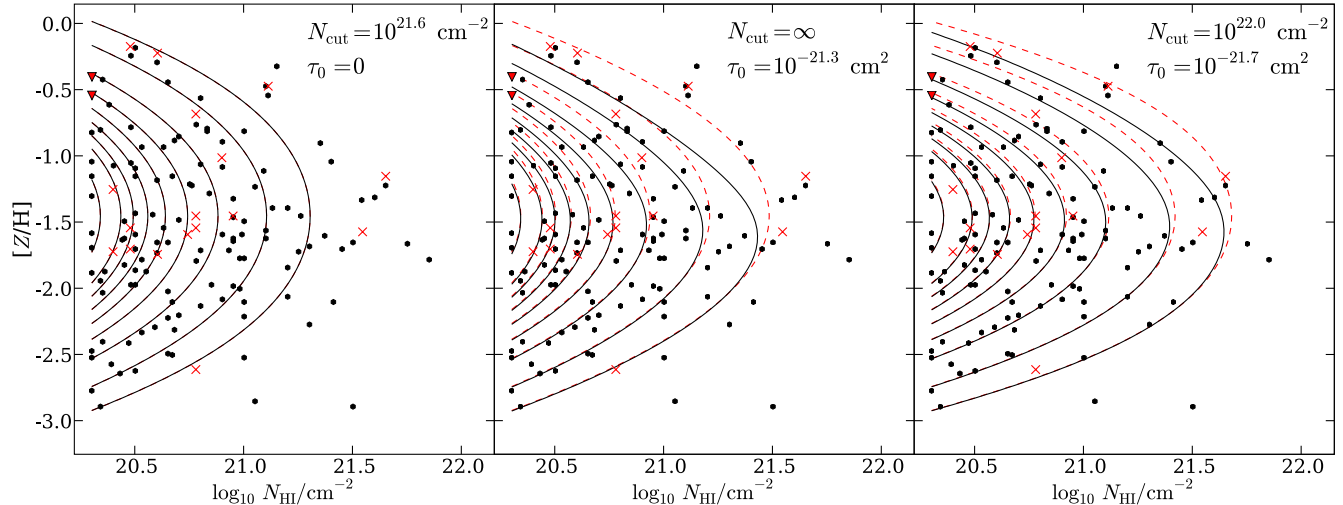


Figure 1. A heuristic picture of different regions of our model space. Our optical sample based on Dessauges-Zavadsky et al. (in prep.) is shown by dots; the CORALS radio sample based on Akerman et al. (2005) is shown by crosses or triangles for the upper limits (see Section 2.2 for a discussion of these datasets). Contour lines of equal probability density in the $\log N_{\text{HI}} - \log Z$ plane for finding a DLA in an optical sample (solid lines) or radio sample (dashed lines where this differs from the optical case) are shown for three models. In each panel, the contours correspond, from left to right, to 0.9, 0.8, . . . , 0.2, 0.1 and 0.05 times the peak probability density. In the left panel, high column densities of hydrogen are intrinsically unlikely but there is no dust absorption; in the central panel, the Schechter-type intrinsic cut-off is absent, but dust truncates the observed high column densities of metals. The final panel illustrates the favoured type of model from our analysis, in which both intrinsic and obscuration mechanisms have some part to play in shaping the optically observed distribution. By eye, the three sets of optical contours appear similar; this illustrates the need for a rigorous method to probe the role of dust in shaping the final distribution.

Thus statistical interpretation of these apparent trends must be approached with care.

In fact, a range of constraints cast doubt on models predicting a substantial bias. Starting from the observed relative abundances of elements which are depleted onto dust by differing amounts such as zinc (undepleted) and chromium (severely depleted), Pettini et al. (1997) estimated a DLA-induced extinction at 1500Å of just ~ 0.1 mag. More directly, samples of radio-selected QSOs (which are unaffected by dust) exhibit similar incidence rates of DLAs as their optical counterparts (Ellison et al. 2001; see also Jorgenson et al. 2006, although the optical identification in this latter work is not complete). Moreover, high resolution spectroscopy of the Ellison et al. DLAs (known as the CORALS sample) shows a similar distribution of metal column densities as found in optical samples (Akerman et al. 2005). While the radio-selected samples do show a marginal 1σ difference from the optical data in both mean metallicity and incidence rate of DLAs (in the correct sense for a dust obscuration bias signature), it is not at all clear whether this is merely a statistical fluke. It is worth noting that, even if the effect on measures such as the incidence rate and mean metallicity is minor, weighted measures such as Ω_{DLA} can be more critically affected. At most risk of being underestimated is the total mass of metals in DLAs, $\Omega_{\text{Z,DLA}}$, which is observationally interesting when conducting a census of metal enrichment over cosmic time (Pettini 2006; Bouché et al. 2007, and references therein).

Overall, the previous work described above appears to be in some tension. Difficulty in understanding these tensions is exacerbated by analyses using ad-hoc statistical methods or “by-eye” assertions. These problems motivated the present work in which we have taken a Bayesian parameter estimation approach to putting useful limits on the effects in question. In our analysis we have used four logically distinct observational datasets: an optically selected

sample of DLAs, a radio selected sample of DLAs, SDSS¹ statistics for the column densities of DLAs, and overall incidence rates for DLAs in radio and optical surveys.

The Bayesian parameter estimation formalism requires us to (i) formulate a parameterized model describing the data and (ii) place prior probabilities on the distribution of parameters for the model. These two processes can, of course, give rise to controversy – especially when the physical processes in play are hard to model. In particular, stage (i) places a unit prior probability on our chosen model: we might humbly admit that this is not entirely satisfactory, but emphasize that the Bayesian technique does not introduce but merely highlights such difficulties. We also performed additional analysis on a widened parameter space which goes some way to mitigating our concerns (see Appendix A). For more details on the Bayesian technique see e.g. Jaynes & Bretthorst (2003).

The remainder of this paper is structured as follows. In section 2.1, we develop a basic model which we argue captures the significant effects of dust-induced obscuration. We describe our use of optical- and radio-selected survey results to calculate likelihoods for this model in section 2.2. With some simple priors described in section 2.3, we examine the resulting statistical estimates for completeness of optical samples in section 3. Finally, we conclude that dust biasing is a real but minor effect in section 4 in which we also discuss how our technique and results differ from similar work by Vladilo & Péroux (2005).

¹ Sloan Digital Sky Survey

2 MODEL AND PARAMETER ESTIMATION

In this section, we will form a simple model for the observed behaviour of absorbers with a continuous parameter which describes the extent to which dust obscuration plays a part. Performing parameter estimation will then allow us to assess the effect of dust absorption on the observed statistics. The final model has five parameters, so we use a Metropolis-Hastings Markov chain Monte Carlo algorithm to sample the posterior probability distribution (Press et al. 2007, and references therein).

2.1 Model

Our simple model starts from the assumption that the intrinsic distribution of DLAs is separable in the (N_{HI}, Z) plane. Although locally N_{HI} and the star formation rate may be expected to be correlated (via the Schmidt-Kennicutt relation observed in local galaxies, see e.g. Kennicutt 1998), our own N -body simulations of galaxy formation (Pontzen et al. 2008), as well as previous simulations (Cen et al. 2003; Nagamine et al. 2004), suggest that there is no significant correlation between N_{HI} and the global star formation history of the host galaxy and hence its metallicity. Thus

$$f_{\text{DLA}}(N_{\text{HI}}, Z) = f_N(N_{\text{HI}}) f_Z(Z) \quad (1)$$

where $f_{\text{DLA}}(N_{\text{HI}}, Z)$ gives the intrinsic probability density of a DLA's location in the (N_{HI}, Z) plane, picked with no observational biases. The distribution of column densities f_N follows a Schechter function (as suggested by Pei & Fall 1995)

$$f_N(N_{\text{HI}}) = N_{\text{HI}}^\alpha e^{-N_{\text{HI}}/N_{\text{cut}}} \quad (2)$$

where α measures the low column density slope and N_{cut} is a characteristic cut-off column density. The distribution of metallicities f_Z is assumed lognormal

$$f_Z(Z) = \frac{1}{Z} \exp\left(-\frac{([\text{Z}] - \mu_Z)^2}{2\sigma_Z^2}\right) \quad (3)$$

where $[Z] = \log_{10} Z/Z_\odot$, μ_Z is the mean log metallicity and σ_Z is the standard deviation of the log metallicity. We have intentionally not normalized our distribution functions at this stage.

These functional forms are based jointly on observational and simulated work – but of course the observations are from magnitude limited optical samples, so it is worth asking whether the intrinsic distributions could in fact have a substantially different shape; we have addressed this possibility in Appendix A (but find that our current parameterization is adequate given some fairly weak assumptions).

2.1.1 Determination of dust column density

We will assume that the optical depth of dust in any system may be modelled as

$$\tau_{\text{dust}}(\lambda, N_{\text{HI}}, Z) = \tau_0(\lambda) N_{\text{HI}} \frac{Z \mathcal{F}_{\text{Fe}}(Z)}{Z_0 \mathcal{F}_{\text{Fe}}(Z_0)} \quad (4)$$

where Z_0 is a normalization metallicity, \mathcal{F}_{Fe} represents the varying fraction of iron in the dust phase as a function of metallicity, and $\tau_0(\lambda)$ specifies a linear scaling between dust column density and optical depth at wavelength λ . This form is based on the fair assumption that the DLA gas density is dominated by the neutral hydrogen density (see Wolfe et al. 2005). Our results are actually rather insensitive to the exact functional form of \mathcal{F}_{Fe} , so long as the fraction in dust increases gently with metallicity, but for ease

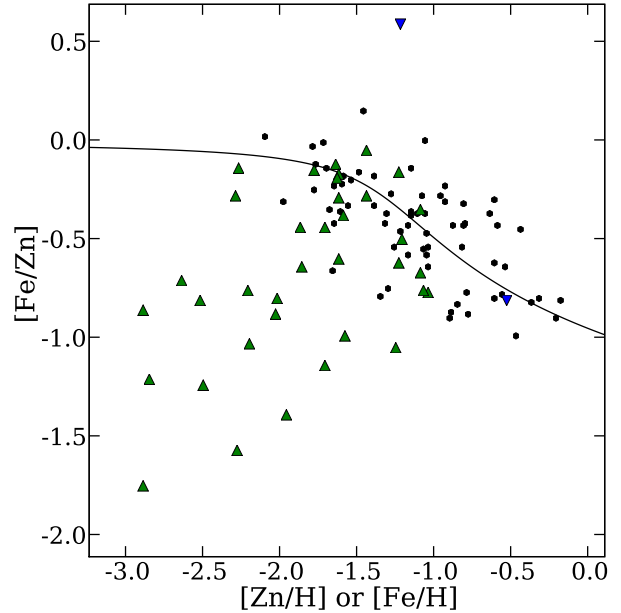


Figure 2. The adopted relation (from Vladilo & Péroux 2005) between the metallicity and fraction of iron in dust is based on the observed relation between metallicity and iron-to-zinc ratio (since zinc does not deplete onto dust grains). Here, data from the optical sample described in the Section 2.2 are plotted (dots and triangles for limits) along with the best fit model (curve).

of comparison we have adopted the form suggested by Vladilo & Péroux (2005):

$$\mathcal{F}_{\text{Fe}} = \frac{1}{2} + \frac{1}{\pi} \tan^{-1} \left(\frac{[Z] - [Z]_0}{\Delta[Z]} \right). \quad (5)$$

Since zinc does not deplete onto dust, the ratio of iron to zinc column densities is predicted by \mathcal{F}_{Fe} :

$$[\text{Fe}/\text{Zn}] \equiv \log_{10} (1 - \mathcal{F}_{\text{Fe}}) \quad (6)$$

This relation can be used, along with observational constraints on iron and zinc abundances in individual systems from the dataset described below in Section 2.2, to estimate best fit parameters² $[Z]_0 = -1.3$ and $\Delta[Z] = 0.48$ in equation (5). For reference, we have plotted this relationship in Figure 2.

2.1.2 Conversion from optical depth to detection probability

We base our predictions for optical samples on the behaviour of a survey for quasars in the SDSS i band with a mean wavelength $\lambda_i \simeq 7480\text{\AA}$. For our optical data (defined in section 2.2 below), the mean redshift $\langle z_{\text{DLA}} \rangle = 3.0$ translates into a DLA rest-frame wavelength of $\lambda_0 = \lambda_i / (1 + \langle z_{\text{DLA}} \rangle) \simeq 1900\text{\AA}$. This will be useful in fixing a prior on τ_0 later. Over the full range of our sample ($1.8 < z < 3.5$) the DLA rest-frame wavelength varies between $1600 < \lambda_0/\text{\AA} < 2700$. According to the low-metallicity extinction law measured in the SMC (Small Magellanic Cloud; Pei 1992),

² We could have included this estimation in our full Bayesian formalism, but due to the insensitivity of our results to the details of the relation $\mathcal{F}_{\text{Fe}}(Z)$, such an approach would add complexity without substantial benefit.

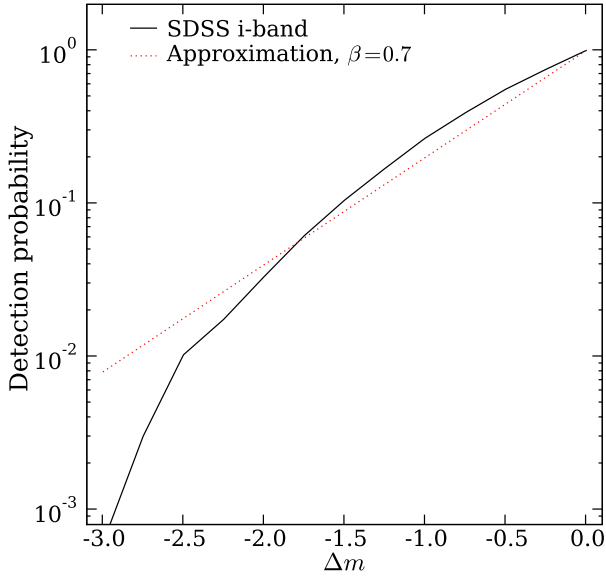


Figure 3. The completeness function for SDSS QSOs in the i band (solid line) compared to our simple analytic approach (dotted line). Δm is the change in the apparent i -magnitude, while the vertical axis shows the fraction of QSOs that would be missed under such a reduction in brightness assuming a step-function sensitivity. The differences between the exact and simple analytic model are only significant when the probability of detection falls below 10^{-2} , and thus have little impact on our overall statistics.

there is a factor two variation in the expected strength of dust absorption over the interval $1600 < \lambda_0/\text{\AA} < 2700$. However, we have chosen not to implement the resulting redshift dependences since:

- (i) the optical metallicity data (section 2.2) are not compiled from a single magnitude-limited sample, but rather from multiple datasets so that an exact modelling is for all practical purposes impossible;
- (ii) computationally, it would be extremely expensive to allow redshift variation (since the normalization of the models would need to be recalculated for every absorber, instead of once per model – see equations 11, 12 below);
- (iii) the stochastic variation in other parameters (metallicity and column density) dwarfs the maximum variation of a factor two; and
- (iv) since the metallicity and column density evolution is known to be weak (Wolfe et al. 2005), systematic biases are unlikely to arise from neglecting slight redshift dependences.

For similar reasons, we do not allow ourselves to become fixated on an exact modelling of the observed quasar background luminosity function. We assume the background population of quasars has an observed distribution in the SDSS i band which obeys $\log_{10} dN/dm = c + \beta m$ with $\beta \simeq 0.7$ (Richards et al. 2006) and that the detection probability is one above a given brightness threshold ($m < m_0$) and zero below ($m > m_0$). Then the total number of quasars which can be observed in the absence of dust obscuration is

$$N_{\text{tot,unobsc}} = \int_{-\infty}^{m_0} 10^{c+\beta m} dm. \quad (7)$$

When dust is introduced, the luminosity of a given system is reduced by a factor $e^{-\tau}$; the apparent magnitude changes by

$\Delta m(\tau) = 2.5\tau/\ln 10$. The number of quasars which could be observed in the presence of such absorption is

$$N_{\text{tot,obsc}}(\tau) = \int_{-\infty}^{m_0} 10^{c+\beta[m+\Delta m(\tau)]} dm \quad (8)$$

so that the probability of detecting a system which has optical depth τ in the i band is reduced by the factor

$$p_{\text{detect}}(\tau) = \frac{N_{\text{tot,obsc}}(\tau)}{N_{\text{tot,unobsc}}} = \exp(-2.5\beta\tau). \quad (9)$$

While emphasis has previously been placed on departures of dN/dm from power law behaviour and hence more complex forms of p_{detect} (Ellison et al. 2004), we find that the actual effects are well modelled by our approach (see Figure 3 which compares the analytic and exact SDSS models). Other than simplicity for its own sake, there is a tangible benefit to keeping the model basic: it can be integrated partially analytically (see Section 2.1.4 below).

2.1.3 Completing the model

The optically observed joint probability distribution $n_{\text{DLA}}(N_{\text{HI}}, Z)$ is simply the product of the intrinsic f_{DLA} with the detection probability p_{detect} ,

$$n_{\text{DLA}}(N_{\text{HI}}, Z) = f_{\text{DLA}}(N_{\text{HI}}, Z) \times \exp\left\{-2.5\beta\tau_0 N_{\text{HI}} \frac{Z \mathcal{F}_{\text{Fe}}(Z)}{Z_0 \mathcal{F}_{\text{Fe}}(Z_0)}\right\} \quad (10)$$

which completes our model. The five free parameters that we have introduced are summarised in Table 1.

In Figure 1 we have illustrated some distributions which can be achieved by the model above. The dotted and solid contours trace respectively lines of constant f_{DLA} (the intrinsic distribution, equation 1) and n_{DLA} (which includes the effect of dust obscuration, equation 10) – i.e. the former traces the distribution of radio-selected DLAs and the latter that of optically-selected DLAs. We have also plotted our optical sample (dots) and radio sample (crosses or triangles for upper limits) on each panel – see Section 2.2 below for details of these datasets. The left panel shows a model where $\tau_0 = 0$ (so no dust obscuration effects are in play). One should note that, despite this, the contours show very small probabilities for high N_{HI} , high Z absorbers simply because the underlying separable distribution $f_N f_Z$ predicts few absorbers in this region. The second panel shows a model similar to that used by Vladilo & Péroux (2005), where no intrinsic cut-off occurs at high N_{HI} , but dust obscuration hides the higher column densities. The third panel shows a combination of these two effects forming the final distribution; our results (Section 3, Figure 4) will show that such a combination is necessary to best describe the data.

2.1.4 Normalization

In assessing our likelihood, we will split the data into two logically distinct constraints: the total density of systems and the distribution of systems within the (N_{HI}, Z) plane. For these purposes, we require the normalizing constants

$$n_0 = \int dN_{\text{HI}} dZ n_{\text{DLA}}(N_{\text{HI}}, Z) \quad (11)$$

$$f_0 = \int dN_{\text{HI}} dZ f_{\text{DLA}}(N_{\text{HI}}, Z). \quad (12)$$

Because of the separability of the intrinsic absorption f , its normalizing constant f_0 may be calculated straight-forwardly to be

Table 1. Summary of parameters and priors thereon for the DLA observation model.

Parameter	Equation	Description	Prior
α	(2)	Low N_{HI} slope	Flat $-2.5 < \alpha < 0$
N_{cut}	(2)	Intrinsic N_{HI} rolloff scale	Flat in log space; $N_{\text{cut}} < 10^{24} \text{ cm}^{-2}$
μ_Z, σ_Z	(3)	Parameters for lognormal metallicity distribution	Flat priors $-3 < \mu_Z < 0; 0.1 < \sigma_Z < 3.0$
τ_0	(4)	Dust optical depth normalization for SMC ($Z_0 = Z_{\odot}/6$)	$\mu = -21.7, \sigma = 1$

$$f_0 = \sqrt{2\pi\sigma_Z} \ln 10 N_{\text{cut}}^{1+\alpha} \Gamma(1 + \alpha, N_0/N_{\text{cut}}) \quad (13)$$

where $N_0 = 2 \times 10^{20} \text{ cm}^{-2}$ is the DLA limiting column density and Γ is the incomplete gamma function,

$$\Gamma(a, x) \equiv \int_x^{\infty} dt t^{a-1} e^{-t} \quad (14)$$

for the evaluation of which we employ a standard numerical algorithm (Press et al. 2007). For the obscured case we integrate analytically over N_{HI} , but the metallicity integral must be performed numerically:

$$n_0 = \int_0^{\infty} dZ f_Z(Z) N_{\text{eff}}^{1+\alpha} \Gamma(1 + \alpha, N_0/N_{\text{eff}}(Z)) \quad (15)$$

$$\text{where } N_{\text{eff}}(Z)^{-1} = N_{\text{cut}}^{-1} + 2.5\beta\tau_0 \frac{\mathcal{F}_{\text{Fe}}(Z)Z}{\mathcal{F}_{\text{Fe}}(Z_0)Z_0} \quad (16)$$

and $f_Z(Z)$ is defined by equation (3).

2.2 Data and Likelihood

Each model is assessed on four points corresponding to properties of optically selected absorbers, properties of radio selected absorbers, a comparison of the line densities of absorbers in these two types of survey and finally SDSS constraints on the column density distribution. The overall likelihood \mathcal{L} is simply the product of the four factors:

$$\mathcal{L} = \mathcal{L}_{\text{opt}} \mathcal{L}_{\text{rad}} \mathcal{L}_{\text{linedens}} \mathcal{L}_{\text{SDSS}} \quad (17)$$

with the terms formally defined below in equations (18 – 22).

We use data from high-resolution optical measurements of 123 DLAs based on the compilation by Dessauges-Zavadsky et al. (in prep.) restricted to the redshift range $1.8 < z < 3.5$ to match the approximate range of the CORALS radio sample (see below)³. For each DLA we use as a measure of its metallicity the zinc abundance relative to the preferred solar value $12 + \log_{10} (\text{Zn}/\text{H})_{\odot} = 4.63$ (from Lodders 2003); where zinc measurements are unavailable we use the iron abundance normalized similarly by $12 + \log_{10} (\text{Fe}/\text{H})_{\odot} = 7.47$. Zinc is not prone to deplete onto dust grains but at lower column densities its transitions become too weak for measurement; conversely, iron is typically disfavoured as a metallicity indicator since it is refractory but the depletion is small at low metallicities (see Figure 2, in which the depletion of iron relative to zinc is plotted). Since our sample is dominated by zinc measurements down to $Z \sim Z_{\odot}/30$, the iron depletion should not be a major concern. In any case, any systematic underestimates of metallicities which may arise would apply equally to radio- and optically-selected DLAs and should therefore not result in any substantive systematic biases for our test.

³ We also checked that we obtained compatible, although slightly less well constrained, final results from the smaller optical sample described by Prochaska et al. (2007).

Observers typically favour targeting high N_{HI} systems for high resolution follow-up. For this reason, we do not allow the distribution of N_{HI} values in the optical metallicity sample to affect our statistics, instead restricting ourselves to measuring the likelihood of each metallicity observation with the column density of the responsible absorber as a given, i.e.

$$\mathcal{L}_{\text{opt}} = \prod_i p_{\text{opt}}(Z_i|N_i) = \prod_i \frac{n(N_i, Z_i)}{\int_0^{\infty} n(N_i, Z) dZ} \quad (18)$$

where i ranges over the optical sample and the final relation follows from the conditional probability rule: $p(Z_i|N_i) p(N_i) = p(Z_i \& N_i)$.

Metallicity data from the radio-selected CORALS survey are taken from Akerman et al. (2005). As for the optical sample described above, we use Zn or (where necessary) Fe to define the metallicity. Unlike the optical case, each radio observation is assessed jointly on its column density and metallicity since no column density biases are expected. For two DLAs no abundances have been measured and for a further two only an upper limit on the metallicity is available. By noting that this situation corresponds to an “infinite upper limit” on the metallicity of the former two DLAs, we can include all systems consistently in the likelihood:

$$\mathcal{L}_{\text{rad}} = \prod_i \frac{f(N_i, Z_i)}{f_0} \times \prod_j \frac{1}{f_0} \int_0^{Z_{\text{max},j}} f(N_j, Z) dZ \quad (19)$$

where i ranges over the radio sample with measured metallicities, and j ranges over those four with only upper limits.

Separately from the (N_{HI}, Z) distribution of observed DLAs, we should also consider the overall incidence rate in optical (e.g. SDSS) and radio surveys. The incidence of DLAs in the SDSS has been discussed extensively for the third data release (DR3) by Prochaska et al. (2005); here we will make use of the updated statistics for DR5⁴.

Because the SDSS pathlength is very much larger than that of any other survey, we make the simplifying assumption that there is no error on its determination of the obscured rate of DLA incidence, $l_{\text{obs}} = 0.063$ over $2.2 < z < 3.5$. This quantity is a measurement of the number density of DLAs per unit “absorption distance” X , defined by $dX/dz = H_0(1+z)^2/H(z)$. The line density of radio-selected quasar DLAs is increased by the ratio of all DLAs to unobscured, i.e. $l_{\text{unobs}} = l_{\text{obs}} f_0/n_0$ (see equations 11, 12). This follows because the line density is at first order proportional to the normalizing constants f_0 and n_0 for the unobscured and obscured cases respectively (see also discussion around equation 23).

We make use of the CORALS (Ellison et al. 2001) results giving a radio sample pathlength of $\Delta X = 195$ (assuming $\Omega_M = 0.3$, $\Omega_{\Lambda} = 0.7$ whence $dX/dz \simeq 3.5$, any errors in which are small compared to sample variance). Although Jorgenson et al. (2006) present additional radio-selected DLA statistics, unlike the

⁴ www.ucoick.org/~xavier/SDSSDLA/DR5/

CORALS results their optical identifications are incomplete and so to be conservative we did not take advantage of the expanded sample. The overall expected number of DLAs in the CORALS sample is λ where

$$\lambda = l_{\text{unobs}} \Delta X = l_{\text{obs}} \Delta X \frac{f_0}{n_0} = 12.3 \frac{f_0}{n_0}. \quad (20)$$

For each model f_0/n_0 and hence λ is determined; given the fixed number of DLAs actually seen in the sample, $k = 17$, the corresponding likelihood is given by the Poisson distribution

$$\mathcal{L}_{\text{linedens}} = \frac{\lambda^k e^{-\lambda}}{k!}. \quad (21)$$

We note that the mean redshift ($\langle z \rangle$) of all DLAs in the two samples (radio and z -limited SDSS) is respectively 2.5 and 2.9. Given the very slow evolution of DLA incidence rate at high redshift, this difference is unimportant.

Finally, the SDSS data produce a joint constraint on the strength of dust absorption τ_0 and the Schechter function cut-off N_{cut} through the distribution of column densities. Because our optical data likelihood \mathcal{L}_{opt} does not take account of the distribution of column densities, the SDSS survey may be regarded as an entirely independent constraint with likelihood

$$\mathcal{L}_{\text{SDSS}} = \prod_i \frac{1}{n_0} \int_0^\infty n(N_i, Z) dZ \quad (22)$$

where i ranges over the 587 systems in the previously described subset of the SDSS DR5 data.

For readers unused to the Bayesian approach to statistics, it may be a surprise that our likelihoods are a product of probability *densities* and therefore will vary under reparameterizations of the data. However the final analysis considers only ratios of probabilities for different models, for which the Jacobian factors cancel.

2.3 Priors

As discussed in the introduction, we are required to place prior probability distribution functions on our parameters to summarise known physics and observational constraints not included in the likelihood. We have little information on DLA dust absorption which is not used in our likelihood analysis, so most of our priors are deliberately as neutral as possible, while limiting the values to reasonable physical expectations.

Note that allowing the column density distribution function cut-off to tend to infinity ($N_{\text{cut}} \rightarrow \infty$) allows for significant numbers of implausibly dense environments. A conservative prior from observations of extreme astrophysical situations (in particular, active galactic nuclei and gamma ray bursts) is that column densities do not exceed $N_{\text{H}} \sim 10^{24} \text{ cm}^{-2}$, which is implemented by adopting a flat log prior for $N_{\text{cut}} < 10^{24} \text{ cm}^{-2}$. In practice, the likelihood is sharply peaked around $N_{\text{cut}} \sim 10^{21.6} \text{ cm}^{-2}$ so that our results are insensitive to this choice.

The parameter controlling the strength of the dust extinction effect, τ_0 , can be estimated. We use the SMC extinction curve (Pei 1992) at our mean rest-frame wavelength $\lambda_0 \simeq 1900 \text{ \AA}$ (see section 2.1 above), gaining $\tau(\lambda_0) = 10^{-21.7} (N_{\text{HI}} / \text{cm}^{-2})$. If we were confident of this estimate, we could fix $\tau_0 = 10^{-21.7} \text{ cm}^2$ and $Z_0 = Z_\odot / 6$ (the SMC metallicity) in equation (4). However, when searching for *direct* evidence of dust obscuration, this would appear circular: τ_0 should be allowed to vary. Z_0 does not need to vary, even if we are unsure of the exact SMC metallicity, since a

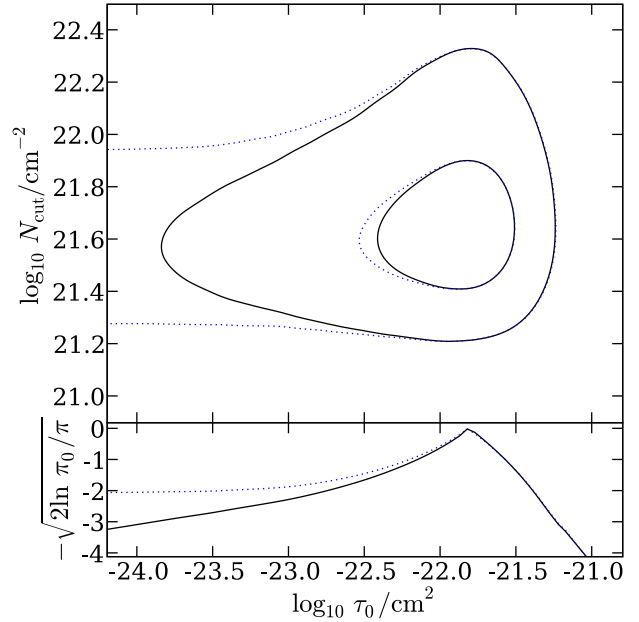


Figure 4. Given the priors on N_{cut} and τ_0 listed in Table 1, the 1 and 2 σ contours for the marginalized Bayesian model fitting problem are shown (solid contours, top panel). These show that our model best fits the observed data when both an intrinsic drop in the number of high column density DLAs and a dust bias are in effect. To illustrate the effect of our prior on τ_0 , the dotted contours are lines of constant probability density for a flat log prior on τ_0 . The lower panel shows the distribution marginalized over N_{cut} to give posteriors on τ_0 .

misestimate can simply be absorbed into the posterior value of τ_0 without affecting the observable predictions of the model.

With our caveat of circularity in mind, it is tempting to try and place some form of uniform prior on $\ln \tau_0$ – but this is impossible, since as the effect tends to zero ($\ln \tau_0 \rightarrow -\infty$), the models become indistinguishable in their predictions for a finite data-set and the likelihood density becomes constant. One must therefore be careful to assign a prior with finite integral as $\ln \tau_0 \rightarrow -\infty$ but which is not so sharp as to exclude the possibility of an unexpected result⁵. This will anyway reflect substantial uncertainties in our estimate of τ_0 (and Z_0). Thus we assign a generous order of magnitude uncertainty at the 1 σ level, making the prior on $\log_{10} \tau_0 / \text{cm}^2$ normal with mean $\mu = -21.7$ and variance $\sigma = 1.0$ dex. The effect of this prior on the results is discussed in more detail in Section 3 below.

We have assigned flat priors to the remaining parameters which control the intrinsic metallicity model and the weak end of the column density distribution (see Table 2). These are well constrained by the data; consequently the priors do not impact strongly on our final results.

3 RESULTS

The result of our analysis is shown in the (τ_0, N_{cut}) plane (marginalized over all other parameters) by the solid contours in the upper panel of Figure 4. These contain 68% and 95% of the total probability, corresponding to 1 and 2 σ limits respectively. We

⁵ Such an unexpected result would likely point to a deficiency in the model.

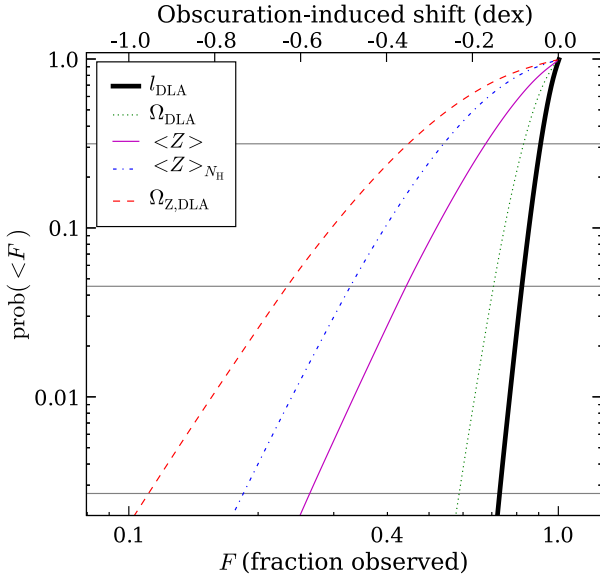


Figure 5. The posterior probability for an optical fractional completeness of at most F is plotted against F for various quantities described in the text (see equations 23 – 27). 1, 2 and 3σ completeness lower limits are given by the intersection of these curves with the grey horizontal lines from top to bottom respectively. Our results show that we are unlikely to miss a substantial number of DLA systems (l_{DLA} is almost complete); however metallicity-weighted measures can be more substantially underestimated (although not by orders of magnitude as previously claimed). See also Table 2.

have shown, in the lower panel, the results of additionally integrating over N_{cut} to gain a completely marginalized distribution for τ_0 . This is plotted as $-\sqrt{2} \ln \pi_0 / \pi$ where π is the posterior probability density in $\log_{10} \tau_0$ and $\pi_0 = \max(\pi)$ is an arbitrary normalization scale. (For a normal distribution, the plotted values $-1, -2, \dots$ would thus correspond to $1\sigma, 2\sigma, \dots$ limits.) The peak in this quantity shows that the posterior distribution strongly suggests dust absorption with the favoured value of $\log_{10} \tau_0 \simeq -21.8$; this is very close to the value estimated earlier for the SMC normalization showing that the model produces results in close accordance with expectations.

However, having used our estimate to place the *prior* on τ_0 , it is legitimate to be concerned that our results simply reflect this prior and hence that the data are not actually constraining the problem. To demonstrate that this is not the case we have also plotted results from assuming a constant log prior on τ_0 (dotted lines in Figure 4). The main peak remains – i.e. it is driven by the likelihood – showing that our prior, as expected, simply cuts off the otherwise infinite distribution as $\tau_0 \rightarrow 0$ (the dotted posterior can be seen to attain a constant value in the bottom panel, and the 2σ contours do not close in the top panel). This confirms the satisfying result that dust obscuration of the strength implied by SMC observations is favoured independently when analysed with our model. We emphasize, however, that the flat prior (dotted contour) results cannot be used in our final assessment for reasons described in Section 2.3. (The dotted contours do not contain a finite probability, but are chosen to correspond to the same probability densities as their solid counterparts.)

3.1 Limits on Optical Completeness

The most important consequence of a dust obscuration scenario is that various cosmological measurements may be biased. In the following, we will express quantities as functionally dependent on the unnormalized distribution function ϕ , where $\phi = f_{\text{DLA}}$ for a radio selected survey or $\phi = n_{\text{DLA}}$ for an optically selected survey. We are particularly interested in the overall incidence rate of DLAs,

$$l_{\text{DLA}}[\phi] \propto \int \phi(N_{\text{HI}}, Z) dN_{\text{HI}} dZ \equiv \phi_0 \quad (23)$$

noting that $\phi_0 = f_0$ for $\phi = f_{\text{DLA}}$ and $\phi_0 = n_0$ for $\phi = n_{\text{DLA}}$; see equations (11) and (12)⁶. Also of interest is the total mass density of neutral hydrogen in DLAs,

$$\Omega_{\text{DLA}}[\phi] \propto \int N_{\text{HI}} \phi(N_{\text{HI}}, Z) dN_{\text{HI}} dZ; \quad (24)$$

the mean metallicity of DLAs,

$$\langle Z \rangle[\phi] \propto \int Z \phi(N_{\text{HI}}, Z) dN_{\text{HI}} dZ / \phi_0; \quad (25)$$

the total mass density of metals in DLAs,

$$\Omega_{\text{Z,DLA}}[\phi] \propto \int Z N_{\text{HI}} \phi(N_{\text{HI}}, Z) dN_{\text{HI}} dZ \quad (26)$$

and the column-density weighted mean metallicity of DLAs,

$$\langle Z \rangle_{N_{\text{HI}}}[\phi] = \frac{\Omega_{\text{Z,DLA}}[\phi]}{\Omega_{\text{DLA}}[\phi]}. \quad (27)$$

Note that the missing constants of proportionality in equations (23 – 26) do not depend on ϕ . For more on the physical significance of these definitions, see Wolfe et al. (2005).

The fractional completeness F of any of these measurements M as measured by an optical survey is defined as

$$F(M) = \frac{M[n_{\text{DLA}}]}{M[f_{\text{DLA}}]} \quad (28)$$

where n_{DLA} and f_{DLA} are the optical and intrinsic distributions, defined by equations (10) and (1) respectively. $F(M)$ depends on our parameters $\vec{r} = \{\alpha, N_{\text{cut}}, \tau_0, Z_0, \sigma_Z\}$; the probability distribution for $Q = F(M)$ is written

$$\begin{aligned} p(< Q_0) &= \int d^5 \vec{r} p(\vec{r}) \theta(Q_0 - Q(\vec{r})) \\ &\rightarrow \sum_{i=1}^N \theta(Q_0 - Q_i) / N \end{aligned} \quad (29)$$

where θ is the Heaviside step function, $p(\vec{r})$ is the posterior probability density, Q is any quantity dependent on the parameters \vec{r} and Q_0 is a value for which the cumulative probability $p(< Q_0)$ is being calculated; when evaluating from the MCMC chain, i ranges over the models in the chain and N is the number of steps. We will also be interested in the expected value of Q ,

$$E(Q) = \int d^5 \vec{r} p(\vec{r}) Q(\vec{r}) \rightarrow \sum_{i=1}^N Q_i / N. \quad (30)$$

The results for the five quantities defined in equations (23 – 27) are shown in Figure 5 and Table 2. For each quantity M , the plot

⁶ Equation (23) assumes that DLAs are lost from optical surveys in direct proportion to $1 - p_{\text{detect}}$, ignoring the second-order effect from the reduction in the number of observed quasars. A full calculation shows that errors introduced by neglecting this term are at the percent level.

Table 2. Expected value of and $1 - 3\sigma$ confidence intervals for various quantities. The first five rows specify the fractional completeness of optical estimates for the specified quantities. The final two rows refer to the expected log mean observable dust absorption specified as the reddening E_{B-V} of the background quasar in the rest-frame of the DLA (see also Figure 6).

Quantity (Q)	$E(Q)$	Confidence Intervals		
		67%	95%	99.7%
$F(l_{\text{DLA}})^{(1)}$	0.93	(0.90, 1.00)	(0.81, 1.00)	(0.72, 1.00)
$F(\Omega_{\text{DLA}})^{(2)}$	0.87	(0.81, 0.97)	(0.70, 1.00)	(0.58, 1.00)
$F(\langle Z \rangle)^{(3)}$	0.75	(0.67, 1.00)	(0.44, 1.00)	(0.26, 1.00)
$F(\langle Z \rangle_{N_{\text{H}}})^{(4)}$	0.63	(0.43, 0.82)	(0.32, 1.00)	(0.18, 1.00)
$F(\Omega_{Z,\text{DLA}})^{(5)}$	0.56	(0.30, 0.75)	(0.22, 0.96)	(0.11, 1.00)
$\log_{10} E_{B-V}$ (optical)	-2.4	(-2.8, -1.8)	(-3.2, -1.8)	(-4.3, -1.6)
$\log_{10} E_{B-V}$ (radio)	-2.1	(-2.5, -1.5)	(-3.5, -1.1)	(-4.5, -0.8)

⁽¹⁾The overall completeness of the optical sample, i.e. the ratio of the line density estimated from optical samples to the intrinsic line density.

⁽²⁾The fractional completeness of optical estimates of the total comoving density of HI in DLAs.

⁽³⁾The ratio of the mean metallicity measured in optical samples to the intrinsic value.

⁽⁴⁾The ratio of the mean column density weighted metallicity measured in optical samples to the intrinsic value.

⁽⁵⁾The fractional completeness of optical estimates of the total comoving density of metals in DLAs.

shows the cumulative probability $p(\text{completeness} < F)$ and the table specifies the expected value $E(F)$ along with confidence intervals at 1, 2, 3σ (i.e. (F_0, F_1) such that $p(F_0 < \text{completeness} < F_1) = 67\%, 95\%$ and 99.7%). The immediate conclusion is that optical samples are likely to be biased but at a level significantly smaller than many previous studies have claimed. Simple quantities such as the overall incidence rates of DLAs (l_{DLA}) are likely to be almost unaffected (with only a 7% expected underestimate and $< 10\%, 19\%$ at 1, 2σ confidence). On the other hand, quantities which are weighted towards higher column densities of metals suffer more from the effects of obscuration. The total DLA mass in HI (Ω_{DLA}) is unlikely to have been underestimated by more than 30% (2σ limit), but a heavily weighted quantity such as the total mass of *metals* in DLAs ($\Omega_{Z,\text{DLA}}$) is underestimated by about a factor of two, or at most 78% (2σ). Note that this nonetheless results in a relatively modest worst-case shift in the mean metallicity of < 0.4 dex (2σ limit) or < 0.5 dex for the column density weighted metallicity (2σ limit).

In some cases, we can compare the completeness limits derived above with analogous estimates by other authors. Trenti & Stiavelli (2006) compared the column density distributions of SDSS DR3 and CORALS radio samples, concluding that optical determinations of Ω_{DLA} underestimated the true value by around 15%, very close to our own expected value of 13%. This is perhaps unsurprising since the information used in this earlier work is a subset of our own dataset. Estimates which take into account the optically determined metallicity distribution (but not the comparison with radio-selected quasars) are to be found in Vladilo & Péroux (2005). The authors give values for the completeness of l_{DLA} of 50–70% and claim Ω_{DLA} is underestimated by at least 50% (their section 6.5). These estimates are inconsistent with our 3σ limits for the minimum completeness, and differ substantially from our expected value of $E[F(\Omega_{\text{DLA}})] = 87\%$. Further, although Vladilo & Péroux (2005) did not give completeness statistics comparable to ours for their metallicity distributions, they suggest metallicities are underestimated by factors of 5 to 6, a shift of about 0.8 dex, again incompatible with our 3σ limits. We explore possible explanations for these differences in Section 4.

3.2 Expected Dust Reddening

Because the optical depth of dust rises rapidly towards shorter wavelengths, observed quasars obscured by dust are expected to exhibit statistically redder spectra than their unobscured counterparts. This effect is discussed in the introduction, but we did not use the results of recent dust reddening studies (Vladilo et al. 2008; Murphy & Liske 2004) as priors in our model, since the uncertainties of these authors' analyses are quite different in nature from the uncertainties in our model. However, we should check that our results are indeed compatible with the observed reddening effect.

We caution that our estimate will assume a proportionality between the colour shift E_{B-V} in the DLA rest-frame and the strength of the overall obscuration, calculated according to the SMC extinction law measured at 1900 \AA . This assumption is not fully justified given the differing DLA redshifts over the sample although, as before, we expect that performing the calculation assuming mean values in this way should not introduce a substantial bias.

The expected reddening effect of a DLA on the background quasar is

$$\langle E_{B-V} \rangle[\phi] = \left(\frac{E_{B-V}}{\tau(1900\text{\AA})} \right)_{\text{SMC}} \tau_0 \times \int dN_{\text{HI}} dZ \frac{N_{\text{HI}} \mathcal{F}_{\text{Fe}}(Z) Z \phi(N_{\text{HI}}, Z)}{\mathcal{F}_{\text{Fe}}(Z_0) Z_0 \phi_0} \quad (31)$$

where the first factor is evaluated from the SMC reddening curve giving $E_{B-V}/\tau(1900\text{\AA}) \simeq 0.12$, the normalizing constant ϕ_0 is defined as usual (equation 23) and $\phi = f_{\text{DLA}}$ for a radio survey or $\phi = n_{\text{DLA}}$ for an optical survey.

The posterior distribution is evaluated according to equation (29) setting $Q = \langle E_{B-V} \rangle$; the results are shown in Figure 6 with confidence intervals listed in Table 2. It is satisfying that our 1σ interval $-2.6 < \log_{10} \langle E_{B-V} \rangle < -2.0$ for an optical survey agrees with the result $\log_{10} \langle E_{B-V} \rangle \simeq -2.2 \pm 0.1$ of Vladilo et al. (2008) (and is consistent with the upper limit of Murphy & Liske 2004). The expected reddening effect of DLAs in radio samples (dashed line in Figure 6) is more pronounced than that in optical samples (solid curve), since the average radio-selected DLA will have a higher column density of metals (no dust bias). This is,

however, compatible with the limit on radio-selected DLA reddening $\langle E_{B-V} \rangle < 0.04$ from Ellison et al. (2005).

3.3 Internal Consistency and Driving Factors

Given that previous studies of the (N_{HI}, Z) evidence for dust obscuration have generally pointed to more pronounced effects than indicated by radio-selected surveys (see Introduction), we should check that this tension is not present in our analysis; if so this could point to a deficiency in the model, limiting the usefulness of the results. A severe tension, with one dataset requiring different parameters from others, would result in the posterior parameters being pushed to intermediate values incompatible with estimates from individual likelihood terms in equation (17).

The optical completeness in our final analysis is expected to be $\sim 90\% - 100\%$ (Table 2), giving an expected number of radio-selected DLAs $11.8 \lesssim \lambda \lesssim 13.1$. Comparing to the actual number, $k = 17$, shows that the radio observations actually detect a slightly larger number than our model has predicted – in other words, they prefer *stronger* dust absorption. However, because of the small path length of existing radio surveys, the Poisson likelihood (21) has a wide variance $\sigma = \sqrt{\lambda} \sim 3.5$. The consequence of this is that the overall 1σ region is almost entirely contained within the 1σ region for the line density data. This shows there is not a substantive tension between these datasets in our analysis. Because of this very consistency (coupled with the wide variance) excluding the line density likelihood from the final analysis makes only minor differences to the results (a fact we explicitly verified); however we have retained it for completeness.

It is worth briefly investigating which data are most powerful in producing constraints on dust effects, especially bearing in mind our comments in the Introduction that the apparent anticorrelation of N_{HI} and Z in optically selected DLA samples can be reproduced without any dust effects whatsoever (see Figure 1). Concretely, our optical sample of zinc and iron metallicities (Section 2.2) is calculated to have a Spearman rank correlation statistic $r = 0.055$, giving a two-tailed p-value of 0.55 (i.e. a sample of the same size with random uncorrelated values will show the same or greater levels of apparent correlation in more than 55% of cases). This leads to the expectation that, on its own, the optical data can place only an upper limit on the effect of dust obscuration. We explicitly verified that this is the case by running our analysis without any radio constraints.

In fact, the major factor in determining our results is the comparison of radio-observed and optically-observed distributions of column densities and metallicities. These lead to the positive *detection* of dust obscuration effects even with neutral priors that allow for no dust in DLAs whatsoever (dotted blue lines in Figure 4; see Section 3). Because this detection so closely matches estimates calculated from observations of the interstellar medium in the SMC, we may have some confidence that our final results are meaningful.

4 DISCUSSION AND CONCLUSIONS

In this work, we have analysed radio- and optically-selected DLA samples to produce an overall picture of dust obscuration. We first noted that the distribution of optically selected DLAs in the (N_{HI}, Z) plane does not point unambiguously to significant dust obscuration. In fact, it is quite possible to form reasonable models in which high metallicity, high H I column density DLAs are rarely

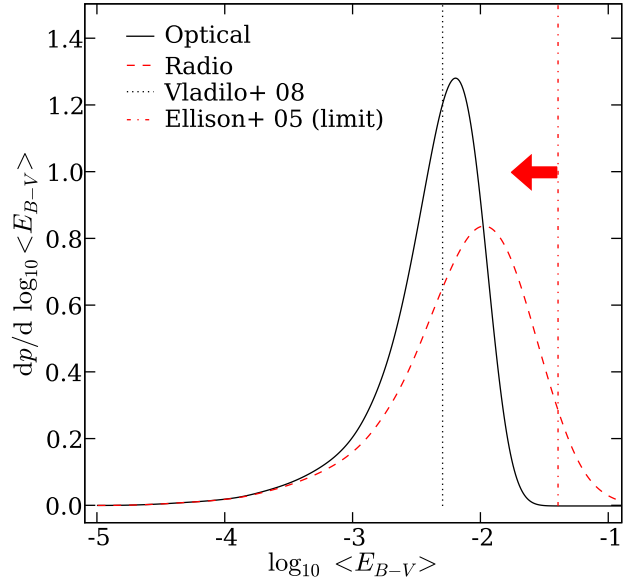


Figure 6. Dust reddening in our models. The solid curve gives the probability density, according to our posterior distribution, of various mean reddenings expected in an optical sample (comparing quasar spectra to their appearance in the absence of a DLA). The dashed curve gives the same statistics for a radio sample (no dust bias). The vertical dotted line gives the measured reddening in SDSS DR5 (Vladilo et al. 2008), while the dash-dotted line gives the direct upper limit on radio-selected quasar reddening derived by Ellison et al. (2005). We emphasize that our model fitting is performed without using any such constraints, so that the agreement of both statistics is an independent validation of our results.

seen simply because the product of the metallicity and column density distributions is small in this region (Figure 1, left panel).

We assembled a simple model of DLA dust obscuration in which the intrinsic DLA distribution is separable in the (N_{HI}, Z) plane and a tuneable dust parameter τ_0 obscures a variable fraction of DLAs from optical samples based on the total column density in dust (modelled as $N_{\text{HI}}Z\mathcal{F}_{\text{Fe}}(Z)$). We then assessed this model using a Bayesian parameter estimation approach with a likelihood based on four sets of observational data: an optically-selected sample of column densities and metallicities (based on Dessauges-Zavadsky et al. in prep.); an equivalent radio-selected survey (CORALS; Ellison et al. 2001; Akerman et al. 2005); the SDSS statistics for observed column densities of DLAs (Prochaska et al. 2005); and a comparison of the incidence rates of DLAs towards optical- and radio-selected quasars (Ellison et al. 2001).

Table 2 summarises the observational predictions of our model. The results do not allow a large hidden fraction of DLAs; thus simple quantities such as their line density (l_{DLA}) are not significantly underestimated in existing surveys. Quantities weighted towards higher metal column densities are (as expected) less well constrained by optical surveys. However, there is still relatively little room for manoeuvre; in particular, our statistics for the metallicity suggest that substantial (i.e. $\gtrsim 1$ dex) dust-induced corrections of the type sometimes invoked to reconcile models with data (e.g. Cen et al. 2003; Nagamine et al. 2004) are not supported by the data.

Our model is similar to that of Vladilo & Péroux (2005; hence-

forth VP05) but we arrive at some qualitatively different conclusions. This may be due to the expanded sample now available, but it is worth noting that our analysis also differs in many details:

(i) We have used a Bayesian approach, being careful to avoid focussing on our peak likelihood model but rather analysing the entire posterior distribution. This leads to well-defined statistical limits on the effects under consideration.

(ii) We have used a substantially larger optical sample of DLAs and additionally considered radio-selected and SDSS observations. We found that on their own optical samples are rather poor at constraining the effects of dust (Section 3.3) whereas adding radio samples returns results which are promisingly consistent with estimates from sightlines through the SMC.

(iii) We formulate the likelihood for each observation rather than simply fitting the distribution using a χ^2 minimization technique. For instance, one may not assume that the statistics of high resolution optical samples trace the underlying N_{HI} distribution since observers choose their targets using a variety of criteria. Such an assumption leads VP05 to estimate a shallower distribution of N_{HI} values than is revealed by the SDSS (powerlaw indices -1.5 and -1.8 respectively), for example. This could plausibly bias the estimation of dust effects.

(iv) We have used a lognormal distribution for metallicity which we argue eliminates some further biases (equation 3 and discussion thereafter, or for more details see Appendix A). Also, we have used iron abundances where zinc are unavailable, since this traces the low metallicity end of the distribution. While iron is refractory and therefore can underestimate true metallicities, this is a small effect at low metallicities where zinc becomes systematically hard to detect (Figure 2). We believe this situation is preferable to ignoring the low metallicity tail of the distribution.

(v) For the column density distribution, we allowed for an exponential cut-off at $N_{\text{HI}} \gtrsim N_{\text{cut}}$ (equation 2). If this parameter were unnecessary, our posteriors would have automatically pushed N_{cut} to high values – but this was not the case (Figure 4). (The likelihood is also sufficiently peaked that only an extreme prior would reverse this trend.) Removing the intrinsic exponential cut-off in N_{HI} would have at least two problematic effects. Firstly, it forces a substantial increase in the deduced effects of dust obscuration, since these alone must account for the drop in observed high N_{HI} absorbers (as illustrated by the central panel of Figure 1). Secondly, it causes estimates for completeness of weighted quantities such as Ω_{DLA} to converge extremely slowly, with a substantial contribution arising from extremely high column densities. VP05 impose arbitrary cut-offs at high N_{HI} to estimate such effects but the results are sensitive to the cut-off chosen.

(vi) We have used a somewhat simplified obscuration model, arguing that fine details are absorbed into our parameter definitions and do not affect estimates for quantities of observational interest.

There are two notable omissions in our modelling. Firstly, we assumed that the intrinsic cutoff N_{cut} was not dependent on metallicity. But taking seriously the suggestion of Schaye (2001) that the physical mechanism for preventing arbitrarily high N_{HI} absorbers is the conversion of H I into H₂, one would expect the characteristic transition column density to be linked to the presence of dust (an essential catalyst in the efficient production of H₂). In fact, this would give a neat explanation for the coincidence of intrinsic and dust-induced cut-offs (by which we mean $N_{\text{cut}} \simeq \tau_0^{-1}$). But if this effect depends on metallicity, as is plausible, it should introduce intrinsic correlations in the (N_{HI}, Z) plane; these would be in the same sense as dust obscuration effects. Since our likelihood is

largely controlled by the comparison of radio and optical data (Section 3.3) which would not essentially be changed in such a scenario, it is likely that our analysis is robust. Nonetheless without a more specific physical model it is hard to assess this in more detail.

Secondly, we have not included a model of gravitational lensing by the host halos of DLAs. There is some evidence in the SDSS sample of a correlation between N_{HI} and the background quasar luminosity which can be explained by this effect (Murphy & Liske 2004; Prochaska et al. 2005). Our simulations (Pontzen et al. 2008) suggest that, in fact, the metallicity Z of a system is a better indication of its mass than N_{HI} . Thus any lensing effect will presumably be correlated with metallicity. If so, the resulting entanglement may cause us to underestimate the dust bias – although if the processes genuinely compensate each other, the completeness limits are unchanged! (Gravitational lensing being monochromatic, this could only work in one waveband.) A full assessment of this possibility awaits future work.

It seems likely that DLA dust biasing is a real but minor effect; all observational constraints are essentially consistent with this conclusion. The fractional completeness of optically-determined values for observable quantities depend on their weighting towards higher metal column densities. The least affected quantity is the overall incidence rate l_{DLA} which is expected to be 93% complete; the most affected quantity is the mass of metals in DLAs $\Omega_{\text{Z,DLA}}$ which is nonetheless expected to be underestimated only by a factor of about two.

ACKNOWLEDGMENTS

We thank Giovanni Vladilo, Celine Peroux, Sara Ellison and the referee, Mike Edmunds, for many helpful comments which improved the quality of this paper. Miroslava Dessauges-Zavadsky, Sara Ellison and Michael Murphy kindly made their compilation of DLA abundances available to us prior to publication; we would also like to acknowledge Chris Akerman, Varsha Kulkarni, Jason Prochaska and their collaborators for making compilations of metallicity measurements in DLAs generally available. AP is supported by a STFC studentship and scholarship at St John’s College, Cambridge and gratefully acknowledges several helpful conversations with Steve Gratton, Natasha Maddox and Antony Lewis.

REFERENCES

- Akerman C. J., Ellison S. L., Pettini M., Steidel C. C., 2005, *A&A*, 440, 499
- Azzalini A., 2005, *Scandinavian Journal of Statistics*, 32, 159
- Boissé P., Le Brun V., Bergeron J., Deharveng J.-M., 1998, *A&A*, 333, 841
- Bouché, N., Lehnert, M. D., Aguirre, A., Péroux, C., & Bergeron, J. 2007, *MNRAS*, 378, 525
- Cen R., Ostriker J. P., Prochaska J. X., Wolfe A. M., 2003, *ApJ*, 598, 741
- Dessauges-Zavadsky M., Ellison S. L., Murphy M. T., in preparation
- Ellison S. L., Churchill C. W., Rix S. A., Pettini M., 2004, *ApJ*, 615, 118
- Ellison S. L., Hall P. B., Lira P., 2005, *AJ*, 130, 1345
- Ellison S. L., Yan L., Hook I. M., Pettini M., Wall J. V., Shaver P., 2001, *A&A*, 379, 393
- Fall S. M., Pei Y. C., 1993, *ApJ*, 402, 479
- Jaynes E. T., Bretthorst G. L., 2003, *Probability Theory*. Cambridge: University Press, 2003.
- Jorgenson R. A., Wolfe A. M., Prochaska J. X., Lu L., Howk J. C., Cooke J., Gawiser E., Gelino D. M., 2006, *ApJ*, 646, 730
- Kennicutt Jr. R. C., 1998, *ApJ*, 498, 541

- Lodders K., 2003, ApJ, 591, 1220
 Murphy M. T., Liske J., 2004, MNRAS, 354, L31
 Nagamine K., Springel V., Hernquist L., 2004, MNRAS, 348, 435
 Pei Y. C., 1992, ApJ, 395, 130
 Pei Y. C., Fall S. M., 1995, ApJ, 454, 69
 Pettini, M. 2006 in V. LeBrun, A. Mazure, S. Arnouts & D. Burgarella (eds.), *The Fabulous Destiny of Galaxies: Bridging Past and Present* (Paris: Frontier Group), p. 319 (astro-ph/0603066)
 Pettini M., King D. L., Smith L. J., Hunstead R. W., 1997, ApJ, 478, 536
 Pontzen A., Governato F., Pettini M., Booth C., Stinson G., Wadley J., Brooks A., Quinn T., Haehnelt M., 2008, MNRAS, accepted (arXiv:0804.4474)
 Press W. H., Teukolsky S. A., Vetterling W. T., Flannery B. P., 2007, *Numerical Recipes: The art of scientific computing*. Cambridge: University Press, 2007, 3rd ed.
 Prochaska J. X., Herbert-Fort S., Wolfe A. M., 2005, ApJ, 635, 123
 Prochaska J. X., Wolfe A. M., Howk J. C., Gawiser E., Burles S. M., Cooke J., 2007, ApJS, 171, 29
 Richards G. T. et al., 2006, AJ, 131, 2766
 Schaye J., 2001, ApJ, 562, L95
 Thomas D., Maraston C., Bender R., Mendes de Oliveira C., 2005, ApJ, 621, 673
 Trenti, M., & Stiavelli, M. 2006, ApJ, 651, 51
 Tytler D., 1987, ApJ, 321, 49
 Vladilo G., Péroux C., 2005, A&A, 444, 461 (VP05)
 Vladilo G., Prochaska J. X., Wolfe A. M., 2008, A&A, 478, 701
 Wolfe A. M., Gawiser E., Prochaska J. X., 2005, ARA&A, 43, 861

APPENDIX A: CHOICE OF FITTING FUNCTIONS

The choice of Schechter and lognormal distribution functions (equations 2 and 3) for our intrinsic column density and metallicity distributions respectively is somewhat arbitrary and we should ensure our choice is as fair as possible given our prior knowledge.

The column density distribution choice is relatively easy to justify. We know that the obscured distribution as uncovered by the SDSS statistics is well fitted by a Schechter function (Prochaska et al. 2005), which consists of a power-law suppressed at high column densities by an exponential decline. This decline can arise due to an intrinsic cut-off (N_{cut}) or due to the exponential dust suppression term in equation (10). We verified that our choice of column density distribution function does not bias our results by using only the SDSS likelihood (equation 22) to produce a posterior prediction for τ_0 which simply returned our prior.

The form of the metallicity distribution presents more serious difficulties. Because of the small-number statistics in the radio samples, we know most about the optically determined (obscured) distribution, which reads

$$n_Z(Z) = \int dN_{\text{HI}} f_Z(Z) f_N(N_{\text{HI}}) p_{\text{detect}}[\tau(N_{\text{HI}}, Z)]. \quad (\text{A1})$$

It should be clear that the intrinsic distribution $f_Z(Z)$ is only recoverable from the data once we know the strength of the dust absorption. Even then, with finite statistics one can never rule out the existence of a population of very high metallicity absorbers which are hidden from view. We therefore need to make an ad hoc parameterization of f_Z which encapsulates our prejudice that (i) the distribution function should change smoothly and (ii) the distribution function is likely to be unimodal. We will not discuss any models which fail to satisfy these conditions, but accept they could change results substantially.

For our main results, we chose to use the lognormal distribution. Vladilo & Péroux (2005) contended that a Schechter function provides a more generic fit, arguing that the shape of the high-

and low-metallicity tails can be independently controlled. However, since both lognormal and Schechter fits have only two parameters, this claim should be interpreted cautiously. Given any two-parameter fit, once the mean and variance are specified the exact distribution function and hence its higher moments (such as the skewness) are fixed. Thus we should investigate which distribution function better encapsulates our knowledge of the systems; if necessary, extra parameters can then be introduced to compensate for deficiencies. The lognormal distribution is a fairly generic choice; further it is supported as a choice for f_Z by simulations (Pontzen et al. 2008) although it is hard to know how much weight to assign to such support.

With our current data we find that the Schechter function provides a very poor representation of the obscured distribution $n_Z(Z)$. Figure A1 (left panel) shows the best fit lognormal and Schechter distributions; with flat priors on the expectation and variance, the latter distribution is disfavoured in log evidence by more than 10, i.e. the probability of the data arising given the latter distribution is more than 20,000 times smaller. Employing this function for the intrinsic distribution $f_Z(Z)$ is therefore likely to bias results against any scenario in which $n_Z \simeq f_Z$, i.e. where dust obscuration is small.

However, accepting that the lognormal distribution may be too restrictive a form for f_Z (even if it fits n_Z well) we investigated the effect of generalising the metallicity distribution to a three-parameter family of distributions which allow for skewing the underlying f_Z . For this purpose, we have used a log skew-normal distribution. The skew-normal distribution (see Azzalini 2005, and references therein) is written

$$\xi(Z; \zeta, M, S) = 2\psi((Z - M)/S) \Psi(\zeta(Z - M)/S) \quad (\text{A2})$$

where ψ and Ψ are respectively the probability density and cumulative probability of the normal distribution. It is remarkable, but simple to show, that this distribution is normalized for all values of ζ . For $\zeta = 0$, the distribution is exactly normal; as $\zeta \rightarrow +\infty, -\infty$ one obtains the half-normal distribution for $Z > M$ and $Z < M$ respectively. In between these extremes, ζ smoothly interpolates between models of varying skewness.

When ζ is allowed to take any value it is possible to find models with large tails of high metallicity DLAs in which dust obscuration makes the optical distribution compatible with the data. An extreme case is illustrated in the right panel of Figure A1; the dashed line shows the intrinsic (strongly skewed) distribution while the solid line shows the observed (dust obscured, nearly symmetric) distribution.

The radio sample is somewhat too small to fully rule out such cases, but we should impose a prior reflecting our knowledge of metallicities in the Universe. In particular, it would be extremely surprising to find a significant number of systems with $Z > 10Z_{\odot}$ (see, e.g., Thomas et al. 2005, in which the centres of $z = 0$ early type galaxies are shown not to exceed even $3Z_{\odot}$). Therefore, in a test run of our markov chain, we allowed ζ to vary with uniform prior but imposed a ‘‘brick wall’’: models predicting greater than one in 1000 intrinsic DLA systems of $Z > 10Z_{\odot}$ were given zero prior probability. This is, of course, an arbitrary choice and will be model-dependent in its implications. But it is a simple first-order approximation, allowing a model with more complex behaviour while imposing our knowledge of direct observations of galaxies.

Comparing this choice with our main ($\zeta = 0$) results, the differences in our posterior distribution were at the percent level and made no difference to our qualitative conclusions presented in the main paper. As the high-metallicity wall is relaxed, allowing

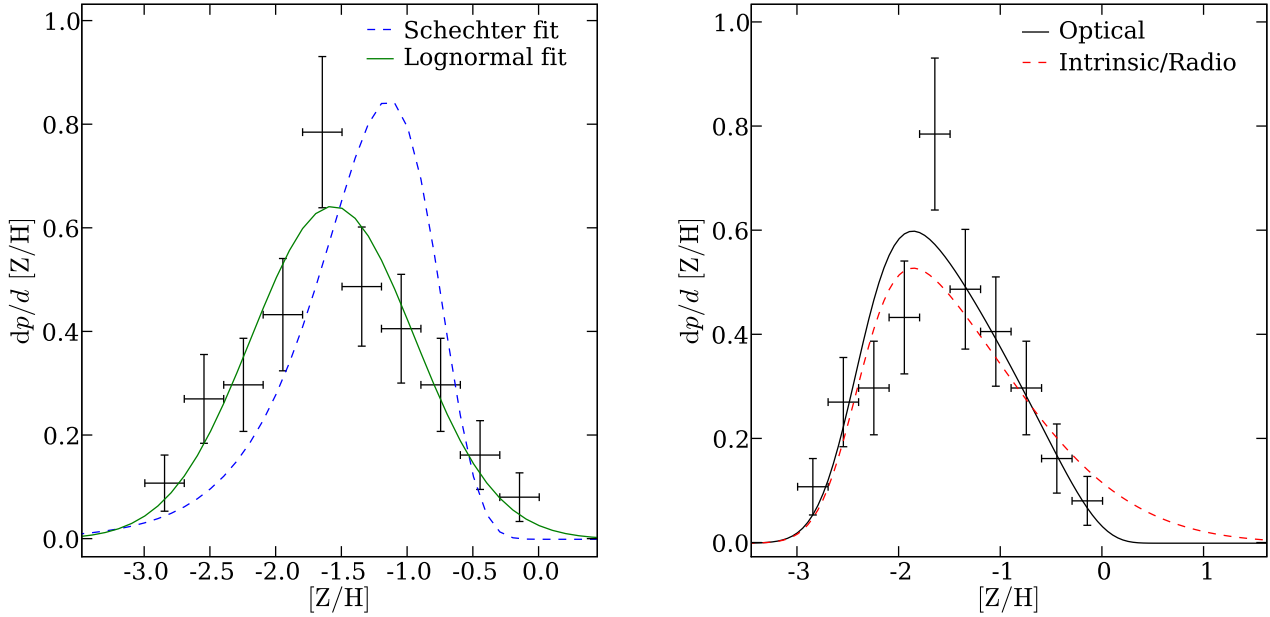


Figure A1. The points with error bars show our optical sample of metallicities based on Dessauges-Zavadsky et al. (in prep.) and described in Section 2.2. (Note that the binning is for illustrative purposes only and is not part of the analysis). In the left panel the solid and dashed lines show simple best fit lognormal and Schechter distributions respectively. The Schechter fit to the observed optical distribution is strongly disfavoured (see text for details) and therefore employing this function for the intrinsic distribution may artificially disfavour small bias scenarios. In the right panel, we illustrate a model in which the underlying metallicity distribution f_Z (shown by the dash line) is strongly skewed in log space, but dust absorption hides the long tail to high metallicities in optically selected surveys (solid line). In the illustrated model, the skewness parameter ζ is 5.8 and the dust obscuration ($\tau_0 = -22.0$) hides the tail almost completely. This model should be discounted by a prior on allowed metallicities – even if the radio sample of DLAs is not strong enough to rule it out, the model includes significant numbers of DLAs with $Z \gg 5Z_\odot$, greater than the values measured in even the most massive galaxies (Thomas et al. 2005).

more $Z > 10Z_\odot$ systems, the constraints are weakened; if one imposes no such prior, allowing systems of arbitrarily high metallicity, 1σ confidence intervals become $0.83 < F(l_{\text{DLA}}) < 0.95$, $0.34 < F(\langle Z \rangle) < 0.69$ and $0.12 < F(\Omega_{Z,\text{DLA}}) < 0.50$. However, we emphasize that much of the obscured cross-section is then in exceptionally high metallicity DLAs with $Z > 10Z_\odot$ – such a model seems very unlikely.

In future, it will be possible to place tighter constraints on these model freedoms by obtaining expanded samples of DLAs from radio-selected QSO spectra. Although further blind radio surveys are relatively slow to reduce the variance of incidence rate statistics (fractional errors for N_{radio} DLAs scale as $1/\sqrt{N_{\text{radio}}}$), high resolution follow-up spectroscopy greatly increases the model-discerning power of the radio observations. Simulations based on our peak posterior model showed that, with an increase in sample size to $N_{\text{radio}} \simeq 35$ (approximately twice the current number of CORALS DLAs with measured metallicities), models with a high-metallicity tail could be independently rejected by the DLA sample. Conversely if a significant high-metallicity skew-normal tail exists but is hidden in optical samples, such a modestly expanded radio sample would be sufficient to reveal its existence. We therefore encourage observers to pursue further searches for DLAs in complete (i.e. fully optically identified) samples of radio-loud QSOs.